BULLETIN OF THE POLISH ACADEMY OF SCIENCES
TECHNICAL SCIENCES, Vol. 73(1), 2025, Article number: e152213
DOI: 10.24425/bpasts.2024.152213

Influence of the metal phase of novel $Al_2O_3/TiO_2/TiAl_2O_5$ composites obtained via the slip casting method

Marcin WACHOWSKI[1], Justyna ZYGMUNTOWICZ[2]*, Robert KOSTUREK[1], Lucjan ŚNIEŻEK[1], Paulina PIOTRKIEWICZ[2], Radosław ŻUROWSKI[3], and Karolina KORYCKA[3]

[1] Faculty of Mechanical Engineering, Military University of Technology, 2 gen. S. Kaliskiego St., 00-908 Warsaw, Poland
[2] Faculty of Materials Science and Engineering, Warsaw University of Technology, 141 Woloska St, 02-507 Warsaw, Poland
[3] Faculty of Chemistry, Warsaw University of Technology, 3 Noakowskiego St, 00-664 Warsaw, Poland

Abstract. This study aims to analyze the ceramic-metal composite $Al_2O_3/TiO_2/TiAl_2O_5$ obtained using the slip-casting method. Samples containing 50% vol. of the solid phase and 2% vol. and 4% vol. fractions of the metallic phase were examined. Rheological investigations were performed. Measurements of shrinkage and density of the composites produced were determined. The phase composition of the obtained composite was investigated using SEM/EDS and XRD techniques. Stereological analysis was performed as well. The slip-casting method enables the production of the proposed composite, reinforced by the presence of TiO_2 and $TiAl_2O_5$. With the increase in the content of the metallic phase in the composite, the thialite phase content increases, but relative density and volumetric shrinkage of the obtained composites both decrease. Thialite grains are characterized by a size in the range of 4 μm to 15 μm, which leads to a low density of the samples. The results revealed that no significant effect of changing the metal phase content of the slurries used for the composites being fabricated was observed on the limiting grain growth of alumina during the sintering process of slip-casting composites. This finding is important as it suggests that the increase in metallic phase content does not lead to undesirable grain coarsening, which could degrade mechanical properties.

Keywords: ceramic matrix; $TiAl_2O_5$; slip casting; composites.

1. INTRODUCTION

The use of ceramic-metal composites in the construction of machines and devices allows for reduction of the weight of selected components while increasing their strength parameters, especially in terms of resistance to abrasion, temperature and to the impact of aggressive environment [1–3]. In recent years, dynamic development of materials engineering has been observed in terms of both the development of new ceramic matrix composites and the improvement of their manufacturing techniques [4, 5]. Depending on the type of reinforcement and its configuration, the material can demonstrate diverse properties [6–10]. Importantly, by setting a different proportion of the metallic phase in the composite, its functional properties can be shaped to a certain extent [11]. The introduction of metallic particles (e.g. aluminum, titanium, nickel) into a ceramic matrix (e.g. Al_2O_3, ZrO_2) makes it possible to obtain a system capable of dissipating energy under conditions of significant load by plastic deformation of metallic particles [12]. In addition, metallic particles are characterized by the ability to block and bridge cracks, which is reflected in the high crack resistance of the composites being considered [12–14]. Due to the relatively low price and favorable mechanical properties, Al_2O_3 is a frequent choice for the ceramic matrix of the composite.

A prospective solution is the introduction of titanium particles into the corundum matrix, whose influence significantly improves the strength parameters of the material produced. Among the methods for producing Al_2O_3-Ti composites, the following can be distinguished: spark plasma sintering (SPS) [15], self-propagating high-temperature synthesis (SHS) [16], high-pressure torsion (HPT) with subsequent annealing [17], and the two-stage process involving slip casting and sintering proposed by the authors in the previous article [18]. As demonstrated in the literature, the manufacturing technique selected significantly determines the strength properties of the composite. For example, the use of high-temperature synthesis (SHS) allowed for the acquisition of an additional share of intermetallic compounds from the Al-Ti system [16]. A similar effect was obtained using high-pressure torsion (HPT) annealing, where the formation of intermetallic compounds and solid solution was reflected in the high hardness of the composite [17]. The two-stage technique of producing the Al_2O_3-Ti composite, proposed by the authors, in the form of slip casting and sintering at 1450°C, allowed us to obtain the proportion of the mixed phase $TiAl_2O_5$ (thialite) [18]. Thialite is a refractory material, and its low conductivity and thermal expansion, together with a relatively high melting point (1860°C), create prospects for obtaining an Al_2O_3-Ti composite with high strength parame-

*e-mail: justyna.zygmuntowicz@pw.edu.pl

Manuscript submitted 2024-02-27, revised 2024-10-01, initially accepted for publication 2024-10-03, published in January 2025.

ters at high temperatures [19]. Slip casting is a relatively cheap method for the production of items with complex shapes, e.g. gas turbine rotors. Due to the fact that casting in single molds is usually labor-intensive, battery casting is used to produce multiple pieces at once. In this method, the molds are assembled into units and filled with slurry all at the same time. It should be borne in mind that in the slip casting method, the starting materials used in the production process have a huge impact on the final microstructure and, consequently, the properties of the material. In addition to the raw materials used in the manufacturing process, an equally important parameter affecting the final product is the composition of individual components, including metallic components in the metallic phase. Despite demonstrating the possibility of obtaining a composite reinforced with thialite by slip casting and sintering, there is still the problem of accurately determining the influence of the slurry composition on the casting properties and strength parameters of the target composite. The slip composition significantly affects its rheological properties, which is an important factor in the slip casting technique [20]. The strength properties of composites will be largely determined by the participation of the metallic phase and additional reinforcing particles (intermetallic compounds, thialite) [21, 22].

The work is a continuation of research on the production of a composite from the Al_2O_3-Ti system with optimal properties and microstructure, with the largest possible share of an additional phase in the form of thialite. The results of preliminary studies on the Al_2O_3-Ti composite produced by slip casting were published by Wachowski *et al*. [18]. The previously published work presented initial research results on manufacturing this type of composite. The focus was on the manufacturing and analysis of composite from the Al_2O_3-Ti system, which contained 50% vol. of the solid phase, including 10% vol. of the metallic phase. The article applied the original concept of formation (i.e. method, parameters) of ceramic matrix material enhanced by the thialite phase. The rheological characteristics of ceramic suspensions made from Al_2O_3 and Ti were examined. Thermogravimetric analysis was performed, and the density of the sintered samples was ascertained through the use of the pycnometer method. In order to determine the phase composition of the fittings prior to and following the sintering process, XRD and SEM analyses were carried out. The results of the XRD and SEM/EDS analyses indicate that after the sintering process, new TiO_2 and $TiAl_2O_5$ (thialite) phases appeared in the shapes formed. The special properties of $TiAl_2O_5$ make it possible to use this material and composites in many industries. Due to the possibility of obtaining thialite in Al_2O_3-Ti composites, it is necessary to continue research on composites from this system. A previously published paper [17] revealed research results for this composite including only 10% vol. of the metallic phase, which leaves a research gap in a very important aspect about the influence of volume of the metallic phase on the presence and amount of thialite and other phases in Al_2O_3-Ti composites. Therefore, it would be useful to extend the research carried out so far, and thus the subsequent studies, which are the subject of this publication, focused on determining the impact of different participations of the metallic phase (2% vol. and 4% vol.) on the possibility of producing an Al_2O_3-Ti composite with different participation of the $TiAl_2O_5$ phase. Simultaneously, the idea of the research presented will be used to determine the possibility of forming additional phases in the composites from other systems by means of applying an appropriately modified manufacturing process.

These issues constitute a significant gap in the state of knowledge about the production and properties of new ceramic-metal composites. In this work, the authors focus on slip casting of Al_2O_3-Ti composites with different participations of the metallic phase. The aim of the research and the novelty of this article is to determine both the technological properties of the slurry itself and the basic functional properties of the final composites. The manuscript compares composites containing 50% vol. of the solid phase, containing 2% vol., and 4% vol. of the metallic phase in relation to the total solids content. The process of sintering in an air atmosphere enabled the production of $Al_2O_3/TiO_2/TiAl_2O_5$ composites.

2. EXPERIMENTAL SETUP

In order to produce slips from the Al_2O_3-Ti system containing 50% vol. of the ceramic (solid phase) and 2% vol. and 4% vol. of the metallic phase, an alumina powder with the trade name TM-DAR from Tamei Chemicals Co. (Japan) was used along with titanium powder from GoodFellow Cambridge Limited (England). Table 1 presents the powder specifications as provided by the manufacturers.

Table 1
Specifications of powder used in the research, based on manufacturers' data

Powder	Average powder size	Purity	Density
α-Al_2O_3	100 ± 25 nm	99.99%	3.98 g/cm^3
Ti	75 μm	99.50%	4.51 g/cm^3

The production process of Al_2O_3-Ti composites by casting slips was conducted according to the following steps:

Using a laboratory balance, the ingredients were weighed with an accuracy of up to 0.001 g. The pre-weighed powders were introduced into a blend of water and a fluidizing agent to ensure thorough and uniform mixing of the constituents. Modifying agents were incorporated into the slips during their preparation to achieve the necessary rheological properties. This ensured proper liquefaction of the slips. A combination of liquefying agents was employed, comprising citric acid (CA) and diammonium citrate (DAC). In subsequent sections of the work, citric acid was abbreviated as CA and diammonium citrate as DAC.

The homogenization process was conducted in two stages. In the initial stage, the prepared suspension underwent homogenization using the planetary-ball mill PM 400 (Retsch), a floor model with four grinding stations. The process was carried out for one hour at a rotational speed of 300 rpm. During this homogenization, vessels containing the suspensions were positioned

eccentrically on the rotating base of the planetary ball mill. The base rotated in the opposite direction to the vessels, with a speed ratio of 1:2. The movement of the balls inside the vessels was a result of the Coriolis force, generating high dynamic energy due to the varying velocities between the balls and the vessel. This interaction of friction and impact forces resulted in a significant fragmentation of the ground material. Subsequently, in the second stage, the slurry prepared in the first stage was transferred to a high-speed homogenizer, i.e. THINKY ARE-250, where further homogenization occurred. In the THINKY ARE-250, the initial stage involved mixing for 8 minutes at a rotational speed of 1000 rpm, followed by 2-minute deaeration of the mixture at a rotational speed of 2000 rpm.

The process consists of pouring the slurry (otherwise known as the slip mass) in the form of a powder suspension/mixture of powders in a solvent with additives (fluidizers, wetting agents and surfactants) into a porous mold, usually made of gypsum. Water from the suspension is most often used as a solvent. Under the influence of capillary forces, the liquid medium is drawn into the pores of the mold, thanks to which the slipping mass is compacted, starting at the surface of the mold/slurry boundary. As a result of this process, a negative of the working mold is obtained, into which the slipping mass has been poured. A variant of slip casting was used in the form of double-sided casting to produce the composites, in which special molds consisting of an outer coat and a core were used. The semi-finished products obtained in this manner take their external shape from the shell and the internal shape from the core, so it is possible to control the thickness of the semi-finished product fully.

To achieve flat and parallel surfaces and eliminate shrinkage cavities, the samples were subjected to grinding on sandpaper with varying gradations, including 120, 400, 600, 800 and 1200.

In this experiment, the sintering process took place within an air atmosphere. Table 2 provides an overview of the sintering process parameters. The atmosphere employed allowed for interaction between titanium and oxygen, leading to the production of titanium (IV) oxide (TiO_2). This TiO_2 formation reaction naturally progressed towards oxide formation, as indicated by the negative change in free energy, ΔG. During the subsequent stages of sintering, the titanium (IV) oxide generated had the potential to react with aluminum oxide, resulting in the creation of $TiAl_2O_5$. The sintering process was carried out in the Carbolite chamber furnace of the HTF 17/5 type, model 21-100324, 220 Volt, 50–60 Hz, 19.5 A, 4050 Watt.

Table 2
Stages of sintering of fittings

Sintering stages	Heating	25°C → 1400°C	5°C/min
	Holding	1400°C	120 min
	Cooling	1400°C → 25°C	5°C/min

Two sets of samples were generated from the Al_2O_3-Ti system, each characterized by varying concentrations (2% vol., 4% vol.) of the metallic phase. Slips used for the production of composites contained 50% vol. of the solid phase. In the further part of the work, the samples produced will be referred to as Series I – 2% vol. of the metallic phase (Ti) and Series II – 4% vol. of the metallic phase (Ti).

3. RESEARCH METHODOLOGY

In the first stage of the research, the sedimentation tendency of the slurry masses produced was determined. The primary objective of this study was to validate the stability of the slurry throughout the technological process. The slip is deemed stable if it does not undergo sedimentation within a specified period from the moment it is prepared for use in the mold casting procedure. Two slips from the Al_2O_3-Ti system containing 50% vol. of the solid phase were prepared for suspension stability tests, including, respectively, for Series I – 2% vol. of the metallic phase, and for Series II – 4% vol. of the metallic phase. The suspensions prepared were poured into tightly closed glass containers with the volume of 10 cm^3. Glass containers filled with ceramic slips were positioned on a prearranged measuring platform and underwent macroscopic examinations to detect any settling. Images capturing the condition of the prepared suspensions were captured at 5-minute intervals starting from the commencement of the observation, which was designated as the 0-minute mark. This observation continued for a total duration of 50 minutes.

Viscosity and shear rate measurements over time were conducted using a Kinexus Pro rotational rheometer manufactured by Malvern Instruments in Great Britain. The experiments involved progressively increasing and then decreasing shear rates, ranging from 0.1 s^{-1} to 100 s^{-1} and, subsequently, from 100 s^{-1} to 0.1 s^{-1}. These tests were performed within a plate-plate system with a 0.5 mm gap between the plates, and were conducted at a temperature of 25°C.

In this experiment, the phase composition of the samples was investigated using a Rigaku MiniFlex II diffractometer. Cu Kα radiation with a wavelength of $\lambda = 1.54178$ Å was used. In the experiment voltage $U = 30$ kV, current $I = 15$ mA, angular range $2\theta = 20–100°$, step D$2\theta = 0.01°$ and counting time $t = 1$ second were all used. Diffraction data were compiled using MDI JADE 7 software (Materials Data, Inc.) and the ICDD PDF-4+ 2020 X-ray database.

Using the Archimedes method (standard PN-76/6-06307), apparent density ρ_v, relative density ρ_w, open porosity Po and water absorption N of the obtained sinters were determined.

Linear shrinkage and volumetric shrinkage were determined based on the results of measuring the diameter and height of the samples before and after the sintering process.

To examine the microstructure of the obtained moldings following the sintering process, microscopic investigations were conducted employing a scanning electron microscope (SEM). The observations were made at the fractures of the finished composites. The microstructure tests carried out were aimed at determining how the Ti particles and particles of intermetallic phases were arranged within the matrix. The tests were performed using the JEOL JSM-6610 scanning electron microscope. The examinations were conducted at an accelerated voltage of 15 kV. In order to determine the composition of the distribution of el-

ements in the fittings produced, surface microanalyses of the chemical composition were performed using an Oxford X-Max electro-dispersive spectrometer (EDS). Prior to the examination, a fine layer of carbon was deposited on the samples. In the experiment, a QUORUM Q150T ES sputtering device was applied (Headquarters, Laughton, UK).

Stereological analysis was carried out to assess the impact of the metallic phase content in the slip on the size of Al_2O_3 grains following the sintering process. For this purpose, the MicroMeter v.086b computer program was used [23, 24].

Moreover, utilizing image analysis of the microstructures of alumina grains, the following shape parameters were determined: convexity ($W = p/p_c$), the curvature of grain boundary ($R = p/(\pi \cdot d_2)$) and elongation ($\alpha = d_{\max}/d_2$), The following variables were used in the calculations: p – perimeter of grain [μm], p_c – Cauchy perimeter [μm]), d_2 – diameter of a circle of the same surface as the surface of the examined grain [μm], $d_{\max}$ – maximum diameter of grain projection [μm] [18, 19].

4. RESULTS AND DISCUSSION

4.1. Suspension stability studies

Figure 1 shows photos that reveal the state of suspensions at different time intervals. The tests that were conducted indicated that the suspensions used for composite formation remained stable over time. From the moment the slip was placed in glass containers for 50 minutes, no delamination of the prepared slurries was observed.

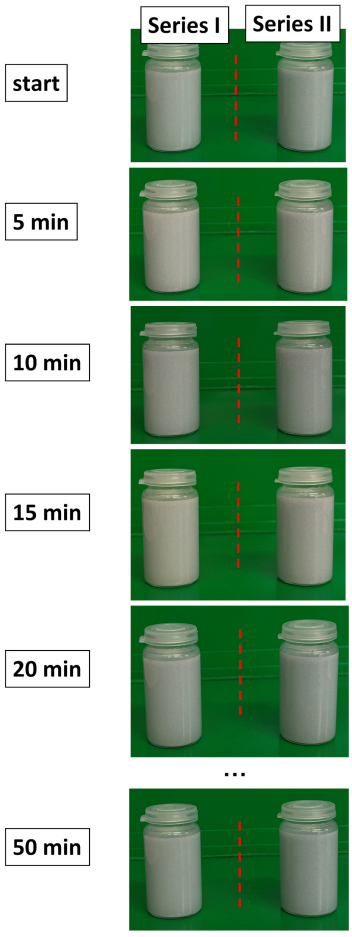

Fig. 1. Sedimentation test of the slurry from the Al_2O_3-Ti system

The subsequent phase of the study aimed to analyze the fundamental rheological properties of the ceramic suspensions produced. The established flow curves (Fig. 2a) and viscosity curves (Fig. 2b) demonstrate that both suspensions exhibit slight thixotropy and display shear-thinning characteristics. In practical terms, this implies that as the shear rate increases during measurement, the dynamic viscosity of both suspensions substantially decreases (as reflected in Table 3). This behavior is attributed to the stacking of slurry components in the direction of flow as stress intensifies. The presented viscosity curve profiles are typical for ceramic suspensions, and the obtained results correlate well with the literature data [25–29]. It is noteworthy, however, that the viscosity curves did not exhibit a minor shear thickening effect within the range of shear rates between 0.1 and 1.0 s^{-1}, as was the case in some of our previous reports describing systems with 50% vol. of the ceramic phase (Al_2O_3 or a mixture of Al_2O_3 and ZrO_2) [30–32]. The reason may be a slightly different composition of the suspension analyzed in this article and, more precisely, the presence of a small amount of the metallic phase (up to 4% Ti) or lack of a binder in the form of polyvinyl alcohol. The results obtained and presented in this paper correspond well with previous reports of the Authors on aqueous suspensions of Al_2O_3/Ni [33] and Al_2O_3/Ti/Ni [21, 34].

Table 3

Dynamic viscosity values for the prepared ceramic slurries at shear rates of 0.1, 1, 10, and 100

Series	Viscosity 0.1 s^{-1} (Pa·s) share rate	Viscosity 1 s^{-1} (Pa·s) share rate	Viscosity 10 s^{-1} (Pa·s) share rate	Viscosity 100 s^{-1} (Pa·s) share rate
Series I	5.21	1.39	0.40	0.16
Series II	7.54	1.72	0.46	0.17

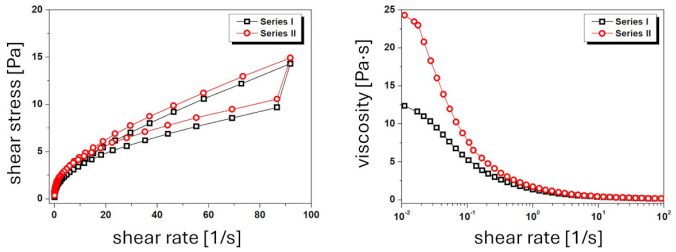

Fig. 2. Flow curves (a) and viscosity curves (b) of the prepared ceramic slurries: Series I – 2% vol. Ti, Series II – 4% vol. Ti

Analyzing the data presented in Fig. 2b further, it is also worth noting the significant differences in the viscosity of the suspensions from Series I and Series II, visible particularly in the range of low shear rates. The suspension containing 4% vol. Ti has almost twice as high viscosity as compared to the system containing 2% vol. Ti. As in our previous publication [34], this

fact can be explained by the presence of relatively large irregularly shaped titanium particles, which have the most significant effect on the viscosity of the suspension at a low shear rate when these particles are just beginning to align in relation to the flow direction. The effect of a much higher viscosity is, of course, stronger in the case of a higher content of titanium.

4.2. Determination of selected properties

The physical properties of samples containing 50% solid phase, with 2% and 4% metallic phase, were determined using the Archimedes method. These results are shown in Table 4. It was observed that increasing the metallic phase reduced relative density of the composites. For Series I (2% Ti), relative density was 98.25 ± 0.22%. In Series II (4% Ti), the density decreased to 96.10 ± 0.88%. Tests revealed that lowering the sintering temperature by 50°C (from 1450°C to 1400°C) worsened densification [18]. Earlier studies reported a density of 99% when sintering was conducted at 1450°C [18]. The lower density in this study may be due to the formation of new phases during the sintering process. These new phases, likely TiO_2 and $TiAl_2O_5$, will be confirmed through XRD analysis. Open porosity was also measured: 0.38 ± 0.14% for Series I and 2.29 ± 0.34% for Series II. Water absorption in both series was below 1%.

Table 4
Physical properties of the composites

		Series I – 2% vol. of the metallic phase	Series II – 4% vol. of the metallic phase
Theoretical density	[g/cm^3]	4.002	4.0104
Relative density	[%]	98.25 ± 0.22	96.10 ± 0.88
Open porosity	[%]	0.38 ± 0.14	2.29 ± 0.34
Water absorption	[%]	0.09 ± 0.04	0.63 ± 0.09

4.3. Determination of volumetric and linear shrinkage of the samples produced

The results in Table 5 indicate that samples with more metallic phases have lower volumetric shrinkage. Series I and Series II show a slight difference in linear shrinkage measured along the height. The linear shrinkage values along the height are within error limits. For Series I, linear shrinkage at height was 10.63%. For Series II, it was 11.13%. There were differences in linear shrinkage along the diameter between the series. Series I, with less metallic phase content, exhibited higher linear shrinkage, a trend also seen in volumetric shrinkage. The volumetric shrinkage for Series I was 31.47%. For Series II, it was 28.39%.

Table 5
Shrinkage of the obtained composites

		Series I – 2% vol. 2% vol. of the metallic phase	Series II – 4% vol. 2% vol. of the metallic phase
Linear shrinkage measured at height	[%]	10.63 ± 0.34	11.13 ± 0.32
Linear shrinkage measured in diameter	[%]	12.35 ± 0.52	10.17 ± 0.45
Volume shrinkage	[%]	31.47 ± 0.25	28.39 ± 0.26

4.4. Composite samples

Figure 3 displays illustrative images of Al_2O_3-Ti fittings fabricated using the slip casting technique. Based on macroscopic assessments of the moldings in their raw, unfinished state, it was determined that the resulting composites exhibit a lack of apparent defects, such as cracks, micro-cracks or surface delamination. The samples before the sintering process have a light blue color, which results from the presence of titanium in the shapes produced. It was observed that following the sintering process, the composites have a light gray color, which may be due to the presence of TiO_2 or/and the $TiAl_2O_5$ phase in the specimens [35].

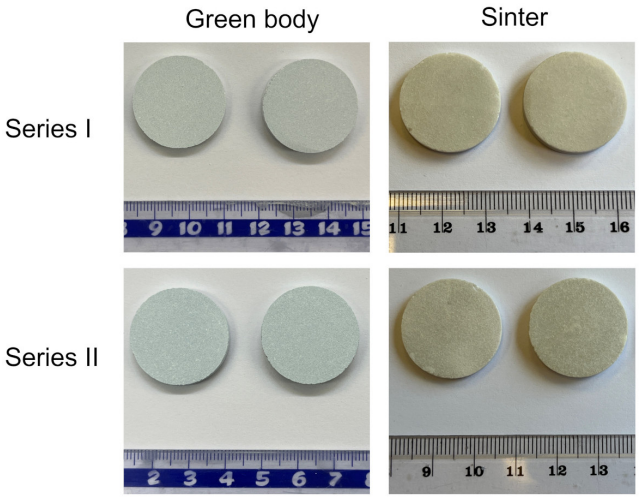

Fig. 3. Example photo of Al_2O_3-Ti composite shapes before and after the sintering process: (a) Series I – 2% vol. of the metallic phase, (b) Series II – 4% vol. of the metallic phase

4.5. XRD phase composition of the raw samples

In the first step, raw samples were analyzed to determine their phase composition. Figure 4 presents the diffractograms of the Al2O3-Ti composites before sintering. XRD analysis revealed the presence of two phases in the samples: α-Al_2O_3 (PDF #01-088-0826) and α-Ti (PDF #00-005-0682). This was consistent across all samples, regardless of titanium content. For samples with 2% titanium (Series I), reflections at 2θ angles of 35.341°, 38.298°, 40.382°, 52.915°, 63.030° and 70.536° corresponded to the following titanium crystallographic planes: (100), (002), (101), (102), (110) and (103). In the 4% titanium samples (Series II), the same titanium crystallographic planes were observed at slightly different 2θ angles: 35.263°, 38.392°, 40.278°, 52.936°, 63.039° and 70.680°.

Subsequently, an X-ray phase analysis was conducted to identify the phases present in the composites that were produced following the sintering process. Figure 5 illustrates the diffrac-

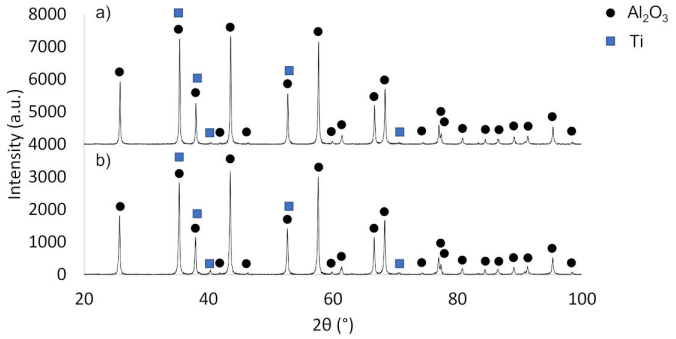

Fig. 4. Diffractograms of Al_2O_3-Ti samples in the raw state: (a) Series I – 2% vol. of the metallic phase, (b) Series II – 4% vol. of the metallic phase

tograms of Al_2O_3-Ti samples after the sintering process. The analysis of the phase composition of the samples after the sintering process in both series confirmed the presence of α-Al_2O_3 (PDF #04-015-8994). The study also revealed the presence of the $TiAl_2O_5$ phase in the structure of the samples produced (PDF #04-007-8576), which is formed as a result of the interphase reaction between Al_2O_3 and Ti during sintering. In addition, TiO_2 peaks were observed in the Series II samples (PDF #98-000-0375). According to the available literature, the $TiAl_2O_55$ phase, the formation of which is thermodynamically favorable for the system, is formed during the sintering of Al_2O_3-Ti composites in the air atmosphere, regardless of the sintering temperature [30].

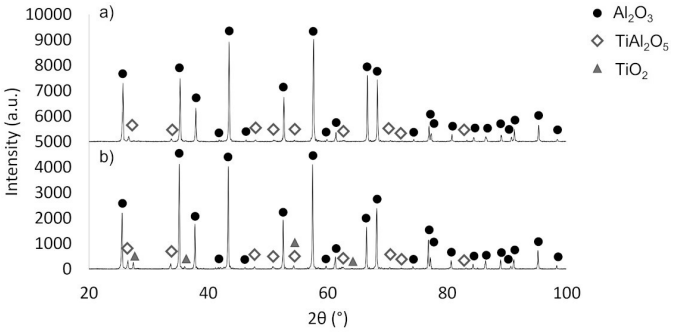

Fig. 5. Diffractograms of Al_2O_3-Ti samples after sintering: (a) 2% vol. of the titanium phase (Series I), (b) 4% vol. of the titanium phase (Series II)

The analysis by direct measurements of the obtained spectra allowed for their characterization. In both series, seven reflections from $TiAl_2O_5$ crystallographic planes were found: (101), (230), (430), (250), (232), (171) and (262). In Series I, the reflections from the same planes were indicated for the 2θ angle values of, respectively: 26.679°, 33.834°, 47.933°, 51.262°, 62.523°, 74.372° and 83.259°, while similarly for Series II, the corresponding values of 2θ angle were equal to: 26.518°, 33.666°, 47.720°, 51.120°, 62.303°, 74.241° and 83.123°. In addition, for Series II, the 2θ angle values corresponding to the reflections from the TiO_2 planes in the diffraction pattern: (110), (101), (211), (310) were equal to, respectively, 27.436°, 36.043°, 54.296° and 64.017°.

4.6. XRD phase composition of the composites

The SEM photos performed in the backscattered electron mode – BSE, as shown in Figs. 6a and 6b, show the characteristic areas of sinters from Series I and II. In the BSE mode, the $TiAl_2O_5$ phase is revealed in a light grey color, and the alumina is shown in a dark grey color. Observations were made at the breakthroughs. SEM studies revealed that the particles of the $TiAl_2O_5$ phase produced are regularly distributed in the Al_2O_3 ceramic matrix, and no areas were observed that are excessively enriched or depleted in the metallic phase. Microstructure analysis confirmed that the particles of the new phase in composites of Series I and Series II have a characteristic microstructure. This phase has a shape similar to an oval with a visible void inside the structure. The presence of voids is an effect of the differences in Al_2O_3, TiO_2, and the $TiAl_2O_5$ thermal expansion coefficients. The obtained microstructure of the $TiAl_2O_5$ phase shown in Fig. 6 is very similar to the microstructure of the $NiAl_2O_4$ – spinel phase of nickel aluminate, obtained in Al_2O_3/$NiAl_2O_4$ composites by pressing and sintering Al_2O_3+Ni powders [36].

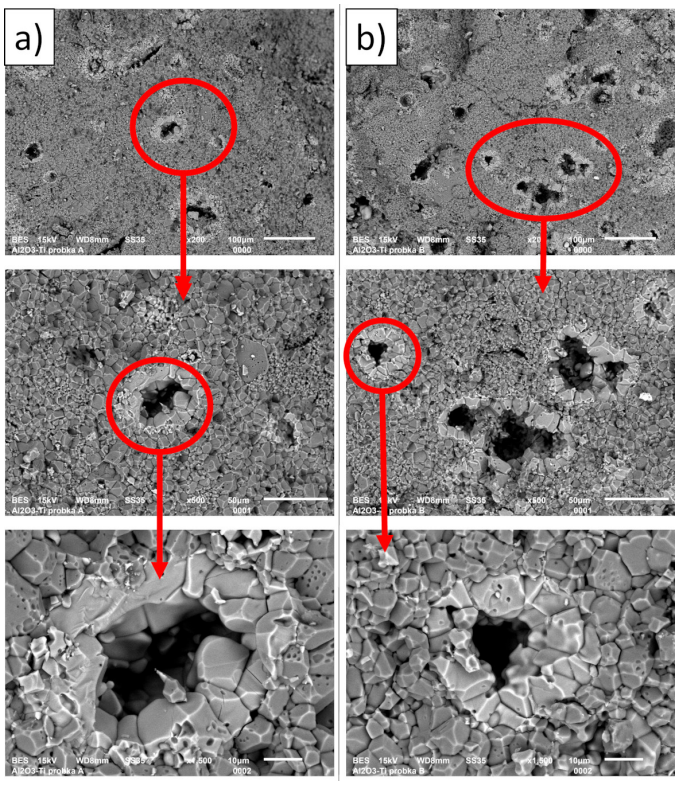

Fig. 6. SEM images of the composites: (a) Series I – 2% vol. of the metallic phase, (b) Series II – 4% vol. of the metallic phase

SEM observations revealed that Series II is characterized by a greater amount of spinel phase than Series I. An increase in metallic phase (titanium) content in the composite results in the increase of the $TiAl_2O_5$ phase content. This observation can be related to density measurement, which indicates that the lowest density was achieved for Series II. The lower density for Series II is mainly due to the morphology of the $TiAl_2O_5$ phase, which is characterized by the presence of voids inside. Moreover, literature data show that a significant problem related

to aluminum titanate is the low strength of the thialite ($TiAl_2O_5$) due to the microcracking phenomenon [37], which leads to a decrease in the density of the composites. L. Giordano *et al.*, in their works, showed that thialite is characterized by very low fracture toughness.

Aluminum titanate decomposes at between 800°C and 1280°C [38]. It remains stable from room temperature up to 750°C, and again from 1280°C to its melting point [37–39]. However, between 750°C and 1280°C, it breaks down into α-Al_2O_3 and TiO_2 [37–39]. During cooling after sintering, extensive microcracks form, which lower both the mechanical strength and density of the material.

Thialite ($TiAl_2O_5$) crystallizes in the orthorhombic space group Cmcm, similarly to pseudobrookite [37, 40]. It exhibits significant anisotropy in its thermal expansion, which leads to thermal hysteresis. This anisotropy is responsible for poor mechanical properties and low density, as it causes severe microcracking during cooling [37, 39].

Remarkably, if the grain size of $TiAl_2O_5$ stays below a critical threshold (1–2 μm), there is insufficient elastic energy to cause microcracks during cooling [41–43]. This significantly improves the material's properties. However, when grain size exceeds this threshold, microcracks increase dramatically. SEM observations showed that the thialite grains ranged from 4 to 15 μm, contributing to the material's low density.

4.7. XRD phase composition of the elements

In the following phase, EDS X-ray spectroscopy was carried out to generate maps illustrating the distribution of elements within the tested samples. The resulting element distribution maps are presented in Fig. 7. In both Series I and II, the presence of aluminum, oxygen and titanium was found. For both sample series, the chemical element distribution maps showed areas enriched in titanium, oxygen and aluminum, which may indicate the presence of an additional $TiAl_2O_5$ phase in these areas. Quantitative analysis of the recorded EDS is presented below.

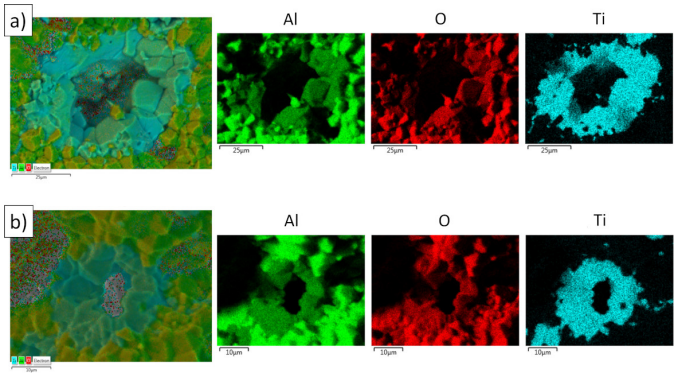

Fig. 7. EDS maps of the composites: (a) 2% vol. of the titanium phase (Series I), (b) 4% vol. of the titanium phase (Series II)

In addition, a spot analysis was carried out to verify the $TiAl_2O_5$ phase areas (Fig. 8). The results obtained are summarized in Table 6. Based on the results obtained, it was found that the measurement points located in the oval areas characteristic of the $TiAl_2O_5$ phase consist of three elements: oxygen, aluminum and titanium, which confirms the presence of the $TiAl_2O_5$ phase. In addition, one measurement was made for each series in the matrix of the composites produced (Series I – point #2, Series II – point #3), which showed only the presence of oxygen and aluminum.

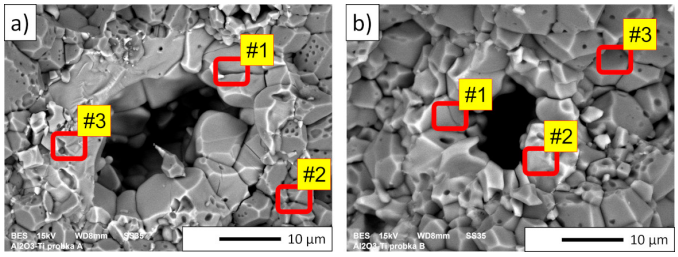

Fig. 8. Points of chemical element distribution in the sample: (a) Series I – 2% vol. of the metallic phase, (b) Series II – 4% vol. of the metallic phase

Table 6

EDS analysis results – the data are shown in weight percentages (wt.%)

Composites series	Point [Fig. 10]	Chemical composition [wt.%]		
		O	Al	Ti
Series I 2 vol.% of the metallic phase	1	46.6 ± 0.2	29.5 ± 0.1	23.9 ± 0.1
	2	43.4 ± 0.16	56.6 ± 0.2	–
	3	39.9 ± 0.2	30.3 ± 0.1	29.8 ± 0.2
Series II 4 vol.% of the metallic phase	1	28.4 ± 1.6	23.8 ± 0.8	47.8 ± 1.3
	2	33.5 ± 1.1	38.9 ± 0.9	27.6 ± 0.9
	3	33.4 ± 3.4	66.6 ± 3.4	–

The SEM images, as shown in Fig. 9 and conducted in BSE mode, reveal distinctive regions of alumina grains in composites produced through the slip casting method. Based on the sample photos presented in Fig. 9, quantitative analysis of the image of aluminum oxide grains for composites was carried out.

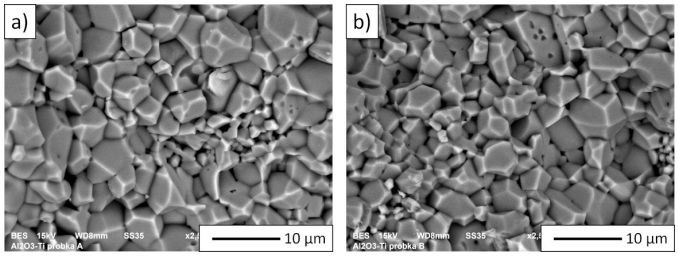

Fig. 9. Microphotography of Al_2O_3 grain size in samples from (a) 2% vol. of titanium phase (Series I), (b) 4% vol. of titanium phase (Series II)

Figures 10 and 11 show the histograms of alumina grain size distribution for both investigated composite series. The histograms indicated that irrespective of the titanium content in the slurries used for the samples being prepared, the specimens showed monoclinic alumina grain size distribution. The results

exhibit that samples from Series I had an average alumina grain size equal to 2.86 μm. Whereas for Series II, the average particle size of the gin oxide was about 2.67 μm. It was found that the obtained alumina grain size values for samples containing a higher metallic phase (Series II) were slightly lower but still within error limits. A study of the histograms exhibited no significant influence of changing the metal phase content of the slurries used for fabricated composites on the limiting grain growth of alumina during the sintering process of slip casting composites. Limiting grain growth refers to the ability to restrict the enlargement of alumina grains during sintering, which is essential for maintaining the desired microstructure. This finding is significant because it indicates that increasing the metallic phase content does not cause undesirable grain coarsening, which could negatively impact the mechanical properties.

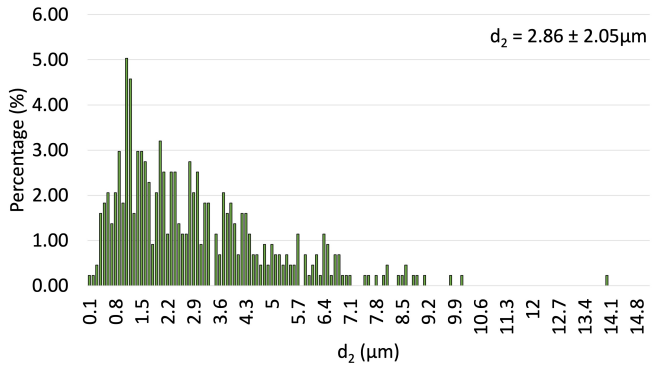

Fig. 10. Histograms of Al_2O_3 grain size in samples from composite with 2% vol. of titanium phase (Series I)

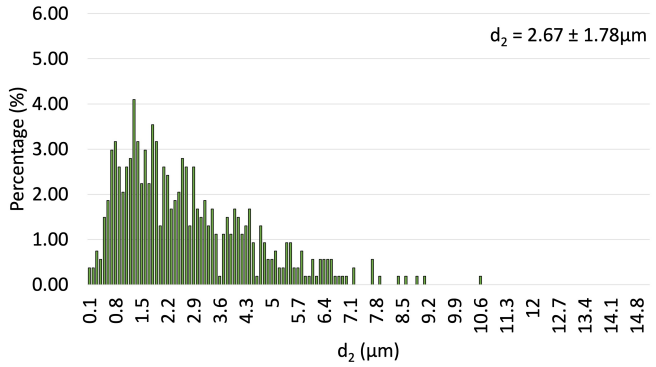

Fig. 11. Histograms of Al_2O_3 grain size in samples from composite with 4% vol. of titanium phase (Series II)

Table 7 presents shape factor parameters describing the alumina in the composites fabricated. According to the obtained results, there was no discernible impact of the titanium phase content on the shape of Al_2O_3 grains. Identical values for shape parameters were observed in both series. Interestingly, similar values of shape parameters for alumina grains were obtained in research on Al_2O_3 matrix composites fabricated via the slip casting method using NiAl-Al_2O_3 composite powder [44].

Table 7
Factors describing shape factors of alumina grains

Series	Convexity $W = p/p_c$	Curvature of the grain boundary $R = p/(\pi d_2)$	Elongation $\alpha = d_{\max}/d_2$
2% vol. of the Ti phase (Series I)	1.08 ± 0.01	1.25 ± 0.02	1.38 ± 0.01
4% vol. of the Ti phase (Series II)	1.08 ± 0.01	1.26 ± 0.01	1.40 ± 0.01

± standard deviation, where: p – perimeter of void [μm], p_c – Cauchy perimeter [μm], d_2 – diameter of a circle of the same surface as the surface of the examined grain [μm], $d_{\max}$ – maximum diameter of void projection [μm] [23, 24].

5. SUMMARY AND CONCLUSIONS

The method of slip casting enables the successful formation of Al_2O_3–Ti composites enhanced with TiO_2 and $TiAl_2O_5$ phases. This method allows for the obtaining of composites with different microstructures, different fractions of additional phases, and their distribution in the ceramics matrix by the addition of different volume fractions of the metallic phase. In this paper, microstructure and properties were investigated for composites obtained with 50% vol. of the solid phase and with different volume fractions of the titanium phase (Series I – 2% vol. and Series II – 4% vol.). Results were compared with previously published research results on similar composites but with 10% of the volume fraction of the titanium phase. That comparison gives a better overview of the possibility of controlling the structure, properties and formation of additional, expected phases in composites from alumina-titanium system obtained by means of the slip casting method. Research revealed (XRD and SEM/EDS) that with the increase of the volume fraction of the metallic phase in the composite, the content of the $TiAl_2O_5$ and TiO_2 phases increases. The properties of the composite undergo changes depending on the content of the metallic phase, indicating a discernible dependence. A higher amount of metallic fraction used in production results in the decrease of relative density and volumetric shrinkage of the composites (measured by the Archimedes method). The microstructure of the thialite phase is characterized by the presence of voids that influence the decreasing final density of the composite. The investigation revealed that altering the metallic phase content in the slurries employed for fabricating composites had no significant impact on the limiting grain growth of alumina during the sintering process in slip-casting samples. Limiting grain growth refers to the capacity to prevent the enlargement of alumina grains during sintering, which is crucial for preserving the desired microstructure. The research findings contribute to the advancement of knowledge regarding the technological aspects of manufacturing composites from the Al_2O_3-Ti system. They provide insights into the interplay between metallic phase content, structure, chemical and phase composition, and the fundamental properties of the resultant composites. These results enhance comprehension of the technological processes involved in producing composites through the slip-casting method. Consequently, they establish

the foundational principles that can serve as a starting point for developing ceramic-metal composites in other systems.

6. CONCLUSIONS

Based on the research, the following key conclusions can be drawn:

- The slip casting method was effective in producing Al_2O_3/Ti composites reinforced with TiO_2 and $TiAl_2O_5$ phases. This method allows for the creation of composites with varied microstructures, phase compositions and distributions by adjusting the volume fraction of the metallic phase.
- Increasing the metallic phase content (from 2% to 4%) led to a higher content of $TiAl_2O_5$ and TiO_2 phases. This resulted in observable changes in microstructure, with more pronounced thialite ($TiAl_2O_5$) formation.
- A higher metallic phase content resulted in lower relative density and volumetric shrinkage. The presence of voids within the $TiAl_2O_5$ phase contributed to the reduction in density.
- Despite varying metallic phase content, no significant effect on the grain growth of alumina during sintering was observed. Both series displayed similar alumina grain size distributions, with slightly smaller grain sizes in the samples containing a higher metallic phase.
- The research highlights the possibility of tailoring the properties of Al_2O_3-Ti composites by adjusting the metallic phase content, rendering this system versatile for applications requiring specific mechanical and thermal properties.

These findings contribute valuable insights into the influence of metallic phase content on the structural and functional properties of ceramic-metal composites, opening up possibilities for further optimization in industrial applications.

ACKNOWLEDGEMENTS

This research was funded by the Military University of Technology, grant number: UGB/708/2024.

REFERENCES

[1] N. Radhika and M.A. Sathish, "A Review on Si-Based Ceramic Matrix Composites and their Infiltration Based Techniques," *Silicon*, vol. 14, pp. 10141–10171, 2022, doi: 10.1007/s12633-022-01763-y.

[2] S. Mekalke, J. Kendannavar, and R. Rao, "Performance Testing of Ceramic Metal Composites: A Review," *I-manager's J. Mater. Sci.*, vol. 7, no. 4, pp. 42–50, 2020, doi: 10.26634/jms.7.4.15866.

[3] M. Lou *et al.*, "Temperature-induced wear transition in ceramic-metal composites," *Acta Mater.*, vol. 205, p. 116545, 2021, doi: 10.1016/j.actamat.2020.116545.

[4] X. Ji, C. Zhang, and S. Li, "In Situ Synthesis of Core-Shell-Structured SiCp Reinforcements in Aluminium Matrix Composites by Powder Metallurgy," *Metals*, vol. 11, p. 1201, 2021, doi: 10.3390/met11081201.

[5] U. Scheithauer, T. Slawik, E. Schwarzer, H.J. Richter, T. Moritz, and A. Michaelis, "Additive Manufacturing of Metal-Ceramic-Composites by Thermoplastic 3D-Printing (3DTP)," *J. Ceram. Sci. Technol.*, vol. 6, pp. 125–132, 2015, doi: 10.4416/JCST2014-00045.

[6] I.M.R. Najjar, A.M. Sadoun, M. Abd Elaziz, H. Ahmadian, A. Fathy, and A.M. Kabeel, "Prediction of the tensile properties of ultrafine grained Al–SiC nanocomposites using machine learning," *J. Mater. Res. Technol.*, vol. 24, pp. 7666–7682, 2023, doi: 10.1016/j.jmrt.2023.05.035.

[7] E. Ghandourah *et al.*, "Comprehensive investigation of the impact of milling time on microstructural evolution and tribological properties in Mg-Ti-SiC hybrid composites," *Mater. Today Commun.*, vol. 38, p. 107835, 2024, doi: 10.1016/j.mtcomm.2023.107835.

[8] W.S. Barakat, M.I.A. Habba, A. Ibrahim, A. Fathy, and O.A. Elkady, "The effect of Cu coated Al_2O_3 particle content and densification methods on the microstructure and mechanical properties of Al matrix composites," *J. Mater. Res. Technol.*, vol. 24, pp. 6908–6922, 2023, doi: 10.1016/j.jmrt.2023.05.010.

[9] A.M. Sadoun *et al.*, "An enhanced Dendritic Neural Algorithm to predict the wear behavior of alumina coated silver reinforced copper nanocomposites," *Alex. Eng. J.*, vol. 65, pp. 809–823, 2023, doi: 10.1016/j.aej.2022.09.036.

[10] I.R. Najjar, A.M. Sadoun, A. Fathy, A.W. Abdallah, M.A. Elaziz, and M. Elmahdy, "Prediction of Tribological Properties of Alumina-Coated, Silver-Reinforced Copper Nanocomposites Using Long Short-Term Model Combined with Golden Jackal Optimization," *Lubricants*, vol. 10, no. 11, p. 227, 2022, doi: 10.3390/lubricants10110277.

[11] P. Singh, N. Ram Chauhan, and S. Rajesha, "Effect of the addition of ductile phase on mechanical properties of Alumina/nano SiC ceramic composite," *Adv. Mater. Process. Technol.*, 2022, doi: 10.1080/2374068X.2022.2120291.

[12] K. Konopka, M. Maj, and K.J. Kurzydłowski, "Studies of the Effect of Metal Particles on the Fracture Toughness of Ceramic Matrix Composites," *Mater. Charact.*, vol. 51, pp. 335–340, 2023, doi: 10.1016/j.matchar.2004.02.002.

[13] Y. Zhang, and X. Li, "Bio-inspired, Graphene/Al_2O_3 Doubly Reinforced Aluminum Composites with High Strength and Toughness," *Nano Lett.*, vol. 17, pp. 6907–6915, 2017, doi: 10.1021/acs.nanolett.7b03308.

[14] W. Fahrenholtz, D. Ellerby, and E. Loehman, "Al_2O_3–Ni Composites with High Strength and Fracture Toughness," *J. Am. Ceram. Soc.*, vol. 83, no. 5, pp. 1279–1280, 2000, doi: 10.1111/j.1151-2916.2000.tb01368.x.

[15] S. Meir, S. Kalabukhov, N. Frage, and S. Hayun, "Mechanical Properties of Al_2O_3\Ti Composites Fabricated by Spark Plasma Sintering," *Ceram. Int.*, vol. 41, pp. 4637–4643, 2015, doi: 10.1016/j.ceramint.2014.12.008.

[16] D. Horvitz, I. Gotman, E. Gutmanas, and N. Claussen, "In Situ Processing of Dense Al_2O_3–Ti Aluminide Interpenetrating Phase Composites," *J. Eur. Ceram. Soc.*, vol. 22, pp. 947–954, 2002, doi: 10.1016/S0955-2219(01)00396-X.

[17] K. Edalati, H. Iwaoka, Z. Horita, M. Konno, and T. Sato, "Unusual Hardening in Ti/Al_2O_3 Nanocomposites Produced by High-Pressure Torsion Followed by Annealing," *Sci. Eng. A-Struct. Mater.*, vol. 529, pp. 435–441, 2011, doi: 10.1016/j.msea.2011.09.056.

[18] M. Wachowski *et al.*, "Study on Manufacturing via Slip Casting and Properties of Alumina-Titanium Composite Enhanced by Thialite Phase," *Materials*, vol. 16, p. 79, 2023, doi: 10.3390/ma16010079.

[19] A.M. Segadaes, M.R. Morelli, and R.G.A. Kiminami, "Combustion synthesis of aluminium titanate," *J. Eur. Ceram. Soc.*, vol. 18, pp. 771–781, 1998.

[20] M. Wachowski *et al.*, "Manufacturing of ZrO_2-Ni graded composites via centrifugal casting in the magnetic field," *Bull. Pol. Acad. Sci. Tech. Sci.*, vol. 68, pp. 539–545, 2020, doi: 10.24425/bpasts.2020.133379.

[21] M. Wachowski, J. Zygmuntowicz, R. Kosturek, K. Konopka, and W. Kaszuwara, "Manufacturing of Al_2O_3/Ni/Ti Composites Enhanced by Intermetallic Phases," *Materials*, vol. 14, no. 13, p. 3510, 2021, doi: 10.3390/ma14133510.

[22] M.H. Bocanegra-Bernal and B. Matovic, "Mechanical Properties of Silicon Nitride-Based Ceramics and Its Use in Structural Applications at High Temperatures," *Sci. Eng. A-Struct. Mater.*, vol. 527, pp. 1314–1338, 2010, doi: 10.1016/j.msea.2009.09.064.

[23] T. Wejrzanowski, W.L. Spychalski, K. Rożniatowski, and K.J. Kurzydłowski, "Image based analysis of complex microstructures of engineering materials," *Int. J. Appl. Math. Comput. Sci.*, vol. 18, pp. 33–39, 2008, doi: 10.2478/v10006-008-0003-1.

[24] J. Michalski, T. Wejrzanowski, R. Pielaszek, K. Konopka, W. Łojkowski, and K.J. Kurzydłowski, "Application of image analysis for characterization of powders," *Mater. Sci. Pol.*, vol. 23, pp. 79–86, 2005.

[25] P. Falkowski and R. Żurowski, "Shaping of alumina microbeads by drop-casting of the photopolymerizable suspension into silicone oil and UV curing," *J. Eur. Ceram. Soc.*, vol. 42, no. 9, pp. 3957–3967, 2022, doi: 10.1016/j.jeurceramsoc.2022.03.014.

[26] C.J. Tsai, C.N. Chen, and W.J. Tseng, "Rheology, structure, and sintering of zirconia suspensions with pyrogallol-poly(ethylene glycol) as polymeric surfactant," *J. Eur. Ceram. Soc.*, vol. 33, pp. 3177–3184, 2013, doi: 10.1016/j.jeurceramsoc.2013.06.006.

[27] P. Wiecinski and A. Wieclaw-Midor, "Slip casting of highly concentrated ZnO suspensions: Rheological studies, two-step sintering and resistivity measurements," *Ceram. Int.*, vol. 46, pp. 19 896–19 903, 2020, doi: 10.1016/j.ceramint.2020.05.051.

[28] A. Idzkowska, P. Wiecinska, and M. Szafran, "Acryloyl derivative of glycerol in fabrication of zirconia ceramics by polymerization in situ," *Ceram. Int.*, vol. 40, pp. 13289–13298, 2014, doi: 10.1016/j.ceramint.2014.05.039.

[29] M. Szafran, P. Wiecinska, A. Szudarska, and T. Mizerski, "New multifunctional compounds in gelcasting process- introduction to their synthesis and application," *J. Aust. Ceram. Soc.*, vol. 49, pp. 1–6, 2013.

[30] R. Żurowski *et al.*, "Sustainable ZTA composites produced by an advanced centrifugal slip casting method," *Ceram. Int.*, vol. 48, pp. 11678–11695, 2022, doi: doi: 10.1016/j.ceramint.2022.01.026.

[31] J. Zygmuntowicz *et al.*, "Properties of Al_2O_3-Ti/Ni composites fabricated via centrifugal slip casting under environmentally asessed conditions as a step toward climate-neutral society," *Ceram. Int.*, vol. 48, no. 15, pp. 21879–21892, 2022, doi: 10.1016/j.ceramint.2022.04.174.

[32] R. Żurowski, J. Zygmuntowicz, P. Piotrkiewicz, M. Wachowski, and M.M. Szczypiński, "ZTA Pipes with a Gradient Structure-Effect of the Rheological the Behavior of Ceramic Suspensions on the Gradient Structure and Characterized of the Obtained Products," *Materials*, vol. 14, no. 23, p. 7348, 2021, doi: 10.3390/ma14237348.

[33] J. Zygmuntowicz, A. Miazga, P. Wiecinska, W. Kaszuwara, K. Konopka, and M. Szafran, "Combined centrifugal-slip casting method used for preparation the Al_2O_3-Ni functionally graded composites," *Compos. Part B Eng.*, vol. 141, pp. 158–163, 2018, doi: 10.1016/j.compositesb.2017.12.056.

[34] J. Zygmuntowicz *et al.*, "The Potential of Al_2O_3–ZrO_2-Based Composites, Formed via CSC Method, in Linear Infrastructure Applications Based on Their Mechanical, Thermal and Environmental performance," *Metall. Mater. Trans. A*, vol. 53, pp. 663–678, 2022, doi: 10.1007/s11661-021-06544-7.

[35] S. Shi, S. Cho, T. Goto, and T. Sekino, "The Effects of Sintering Temperature on Mechanical and Electrical Properties of Al_2O_3-Ti Composites," *Mater. Today Commun.*, vol. 25, p. 101522, 2020, doi: 10.1016/j.mtcomm.2020.101522.

[36] J. Zygmuntowicz, A. Miazga, and K. Konopka, "Morphology of nickel aluminate spinel ($NiAl_2O_4$) formed in the Al_2O_3-Ni composite system sintered in air," *Compos. Theory Pract.*, vol. 14, no. 2, pp. 106–110, 2014.

[37] A. Tsetsekou, "A comparison study of tialite ceramics doped with various oxide materials and tialite–mullite composites: microstructural, thermal and mechanical properties," *J. Eur. Ceram. Soc.*, vol. 25, no. 4, pp. 335–348, 2005, doi: 10.1016/j.jeurceramsoc.2004.03.024.

[38] L. Giordano, M. Viviani, C. Bottino, M.T. Buscaglia, V. Buscaglia, and P. Nanni, "Microstructure and thermal expansion of $TiAl_2O_5$–$MgTi_2O_5$ solid solutions obtained by reaction sintering," *J. Eur. Ceram. Soc.*, vol. 22, no. 11, pp. 1811–1822, 2002, doi: 10.1016/S0955-2219(01)00503-9.

[39] M. Nagano, S. Nagashima, H. Maeda, and A. Kato, "Sintering behavior of $TiAl_2O_5$ base ceramics and their thermal properties," *Ceram. Int.*, vol. 25, no. 8, pp. 681–687, 1999, doi: 10.1016/S0272-8842(98)00083-2.

[40] M. Zaharescu, M. Crisan, D. Crisan, N. Drãgan, A. Jitianu, and M. Preda, "$TiAl_2O_5$ preparation starting with reactive powders obtained by sol-gel method," *J. Eur. Ceram. Soc.*, vol. 18, no. 9, pp. 1257–1264, 1998, doi: 10.1016/S0955-2219(98)00051-X.

[41] D.S. Perera and D.J. Cassidy, "Thermal cycling of iron- and magnesium-containing aluminium titanate in a dilatometer," *J. Mat. Sci. Lett.*, vol. 16, pp. 699–701, 1997, doi: 10.1023/A:1018556408965.

[42] Y.X. Huang, A.M. R. Senos, and J.L. Baptista, "Thermal and mechanical properties of aluminum titanate–mullite composites," *J. Mater. Res.*, vol. 15, no. 2, pp. 357–363, 2000, doi: 10.1557/JMR.2000.0056.

[43] T. Yano, M. Kiyohara, and N. Otsuka, "Thermal and mechanical properties of aluminum titanate–mullite composites (part 3) – effects of aluminum titanate particle size," *J. Ceram. Soc. Jpn. Int. Ed*, vol. 100, no. 4, pp. 482–487, 1992.

[44] J. Zygmuntowicz *et al.*, "Characterization of Al_2O_3 Matrix Composites Fabricated via the Slip Casting Method Using NiAl-Al_2O_3 Composite Powder," *Materials*, vol. 15, p. 2920, 2022, doi: 10.3390/ma15082920.